Finite Element Analysis on Induction-balance Magnetic MEMS Sensor

Krishnapriya.S[1], Suja K.J[2], Rama Komaragiri[3]

1. Department of Electronics& Communication, MITS, Varikoli, India
2. Department of Electronics& Communication, NIT Calicut, India
3. Department of Electronics& Communication, Bennett University, Noida, India

Abstract: This paper reports a miniaturized magnetic sensor using an induction-balance setup to detect pathogens or antigens. An analysis is performed using the COMSOL® Multiphysics simulation tool. This novel magnetic particle biosensor consists of non-spiral planar microcoils arranged in induction-balance set up to sense the magnetic particles. The magnetic field lines of the coil are concentrated towards the inner turns, which increases localized particle detection sensitivity of the sensor. A comparison with the existing microcoil configurations is also performed using the finite element features provided by COMSOL. Power consumption is lower than existing structures. The microcoil used is a non-spiral planar microcoil and is similar to a set of parallel short-circuited conductors. The particular field distribution in the non-spiral microcoil helps to reduce magnetic flux leakage with the neighboring components as well. The induction-balance sensor geometry showcases better performance compared to existing planar coil biosensor configurations.

Keywords: Biosensor, Magnetic Particle, Non-spiral planar microcoil, Magnetic flux leakage

Introduction

The significance of portable biomedical instruments such as Lab-on-chip (LoC) devices for point of care testing has increased tremendously nowadays to detect biomolecules such as pathogens, which cause dreadful diseases. The pathogen or any other biomolecules to be detected is called a "target" of the biosensor. In an immunomagnetic assay, a magnetically labeled antibody interacts with the antigen of a pathogen or toxin under detection.

The magnetic labels in biosensors are becoming more popular due to the unique advantages of magnetic sensing techniques. Planar microcoil based magnetic biosensors help to reduce the physical dimensions of the system and improve the sensitivity. The detection of magnetic microbeads is more straightforward, as the test sample does not have any remnant magnetic field. Hence, the magnetic microbeads should be non-remnant or paramagnetic [1]. The beads do not affect the biological interactions in the sample. Moreover, magnetic microbeads won't disintegrate during the processing. Therefore, particle stability is ensured [2, 3].

Biosensors based on magnetic phenomena using planar microcoils can be easily integrated with a microfluidic chip. As a result, the miniaturization of microsensor and improved portability and sensitivity [1, 3]. Therefore, planar microcoil based magnetic sensors are advantageous among the various types of magnetic microsensors. The permanent magnets can be avoided as the microcoil can be used as a source and detector of a magnetic field. The works so far reported on planar microcoil sensors are based on conventional planar spiral microcoils [2, 4, 5].

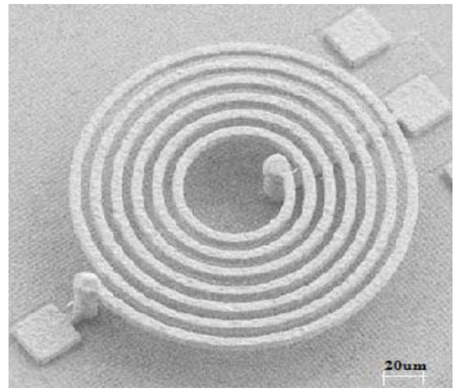

Figure 1. Micrograph of spiral planar microcoil [5]

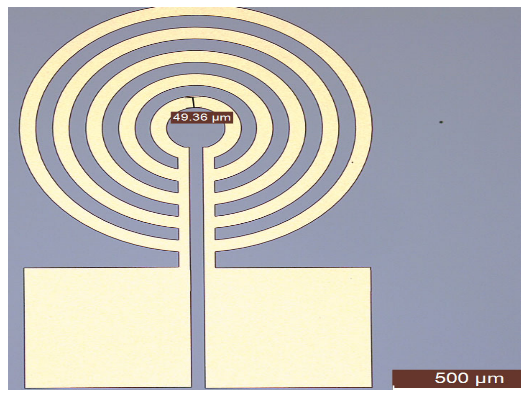

Figure 2. Micrograph of non-spiral planar microcoil

Planar microcoils are primarily categorized as spiral and non-spiral microcoils [6]. In a conventional spiral microcoil shown in Fig.1, as both contact pads are non-coplanar, a metal via is required to connect the center turn to the contact lead. Non-spiral planar microcoil possesses a structure similar to a set of parallel short-circuited conductors leading to a low series resistance of the coil. Non-spiral planar microcoil requires only a single metal layer for microfabrication, as both contact leads are coplanar. This reduced fabrication complexity of non-spiral planar coil along with its lower series resistance, and thereby low Joule heating losses makes non-spiral planar geometry a better alternative over the conventional spiral type. The particular field distribution in the non-spiral microcoil helps to reduce magnetic flux leakage with the neighboring components as well.

In this work, a finite element analysis of a novel magnetic sensor is presented, which is performed using COMSOL Multiphysics simulation software. This novel magnetic particle biosensor consists of non-spiral planar microcoils arranged in an induction-balance configuration to sense the magnetic microparticles [6-8]. The magnetic field lines of the coil are concentrated towards the inner coil turns, which increases localized particle detection sensitivity of the sensor. A comparison with the existing microcoil configurations is also performed using the finite element features provided by COMSOL.

Theory and Simulation Setup

A non-spiral planar microcoil, which is the primary component used for the induction-balance sensor in this work, is simulated first to study the magnetic field distribution within the coil. 2D axisymmetric modeling of the coil is developed using COMSOL, and the simulation domain is shown in Fig.3. Solid rectangular cross-sections in Fig.3 correspond to the coil turns. Coil based physics inside the AC/DC module is used for the modeling, which is generally used to model and solve low-frequency electromagnetic problems.

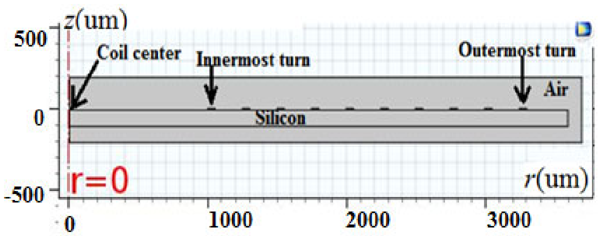

Figure 3. 2D axisymmetric geometry of the non-spiral planar microcoil

Non-spiral planar microcoil is selected as transmitting and receiving coils for the induction-balance sensor. Two transmitting planar microcoils (TX1 Coil and TX2 Coil) and one receiving microcoil (RX Coil) are employed, as shown in Fig.4 to achieve an induction-balance configuration. RX Coil is positioned in such a way to attain primary field suppression in RX Coil's region. By placing two concentric transmitting coils in which exciting currents of equal magnitude flow in opposing directions, a magnetic cavity is created in the region of the receiving coil. RX coil with a radius, *r* is positioned at this cavity region for better sensitivity of detection of the microbeads. The design of the radius, *r,* and details of microfabrication and experimental characterization are discussed in [6, 8].

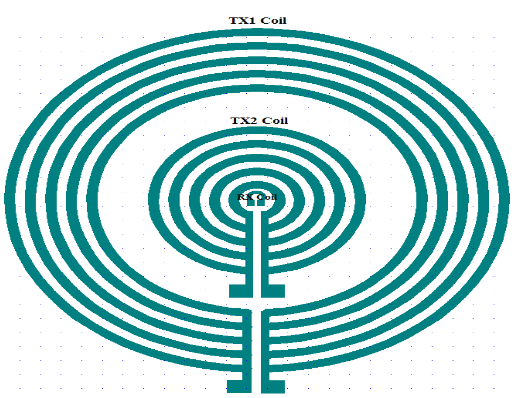

Figure 4. Micrograph of the magnetic sensor in induction balance configuration

The geometrical parameters of the microcoil are listed in Table 1. Here N indicates the number of turns of the coil, w is the width of the coil turn, g is the spacing between adjacent coil turns, and r_1 is the radius of the innermost turn.

Table 1: Geometrical parameters of the induction balance sensor

Coil name	N	w (µm)	g (µm)	r_1 (µm)
TX1	5	50	50	700
TX2	5	50	50	100
RX	1	30	-	20

Governing Equations and Simulation Methods

Magnetic field distribution in a non-spiral planar microcoil takes the form of a Bessel function, as shown in Eq.1.

$$B_z(r,\theta) = \sum_{n=0}^{\infty} a_n J_n(k_c r)\cos(n\theta) \qquad (1)$$

Here a_n is an arbitrary constant, and J_n is the n^{th} order Bessel function.

The sensor geometry is built using 2D axisymmetric modeling in the COMSOL® Multiphysics, as shown in Fig.5 and used to perform finite element analysis of the sensor. AC/DC module is used to performing this sensor simulations. Coil based physics modules are inserted to model the characteristics of the transmitting and receiving microcoils. The current applied to the coils is always in the out-of-plane direction for 2D axisymmetric modeling. Therefore, the capacitive (in-plane) coupling is neglected for this type of model. A homogenized multi-turn option is selected under the coil-based physics module. The conduction current or the induced current is assumed to flow only in the coil turns. The electrical conductivity σ is set to zero in the dielectric regions with no induced current density.

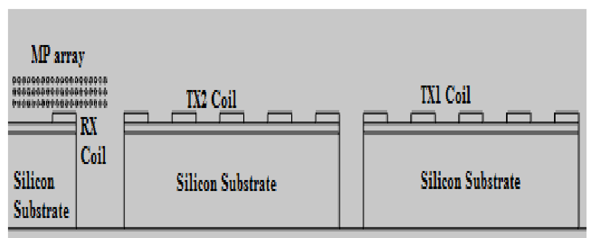

Figure 5. 2D axisymmetric modeling of the induction-balance sensor

At boundaries between the microcoils and air media, the normal component of the magnetic field (B_z) and the tangential component of the electric field (E_r) are continuous. As E_r is continuous across the boundary and zero within the microcoil conductors, E_r is zero at the boundary. As the normal component of magnetic field intensity vanishes within the conductors, B_z is zero at the boundary. Therefore, the tangential electric field and normal magnetic field must be equal to zero at the boundary.

A current, I_{coil}, is applied to the transmitting coils using the "external current density" feature under the "magnetic field" physics, resulting in an external current density. J_e in the direction of the coil turns as per Eq.2.

$$J_e = \frac{N I_{coil}}{A} \qquad (2)$$

Here N is the number of turns that are specified, and A is the total cross-section area of the coil domain.

In the sensor characterization, ferromagnetic microparticles are modeled as circular domains filled with Iron oxide material.

The iron oxide material properties are taken from the Material library feature available in COMSOL. The microparticles or microbeads are shown as MP array in Fig.5. The permeability of the particles is set to 6000. Aluminum is selected as the material for the coil domains, whereas the surroundings are filled with air.

Simulation Results and Discussion

A current of 10 mA is applied at a frequency of 10 kHz considering biomedical sensing applications. Fine physics-based meshing is applied to the geometry, as shown in Fig.6, and the resulting field distribution is shown in Fig.7.

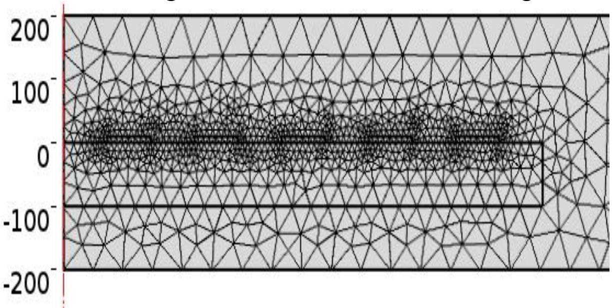

Figure 6. Schematic after meshing

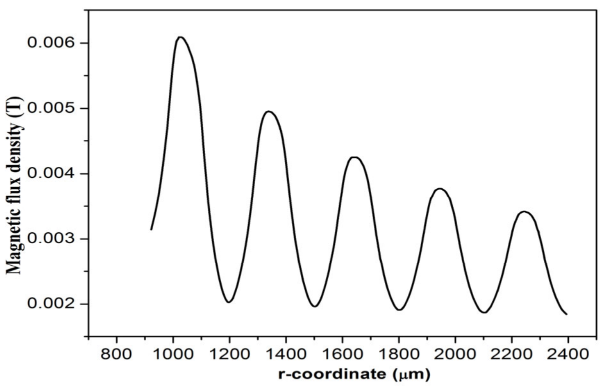

Figure 7. Magnetic flux distribution of non-spiral planar microcoil with five number of turns

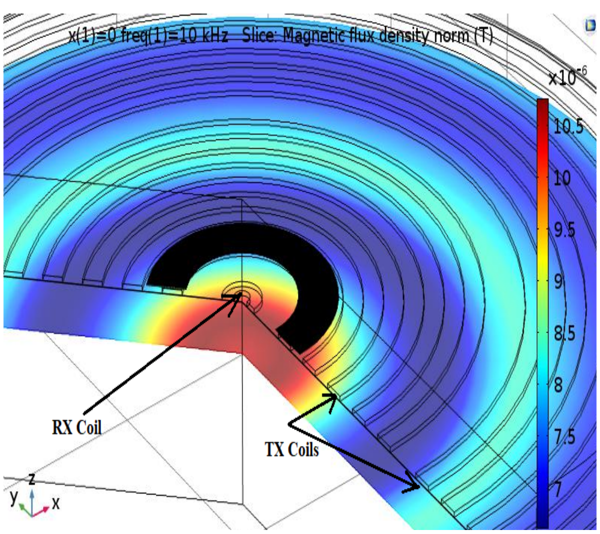

Figure 8. Magnetic flux density distribution in 3D view

The induced magnetic field is observed to be maximum at the edge of the innermost turn, as shown in Fig.7. The field gradually decreases towards outer turns due to the particular current division in non-spiral planar microcoils, which is different from the conventional spiral planar microcoils.

The magnetic field distribution in the sensor is simulated for an input excitation direct current of 100 μA, which is shown in Fig.8. The observed magnetic flux density is of the order of micro Tesla at the interface of microparticle array and exciting coils, as shown in Fig.8 and Fig.9. Magnetic beads near to the inner coil turn of the transmitting coils are magnetized to higher values than those near to the outer turns. The magnetization acquired is of the order of 50 A/m, which is much lower than the saturation level. Saturation levels are of the order of kA/m for iron oxide microbeads [9].

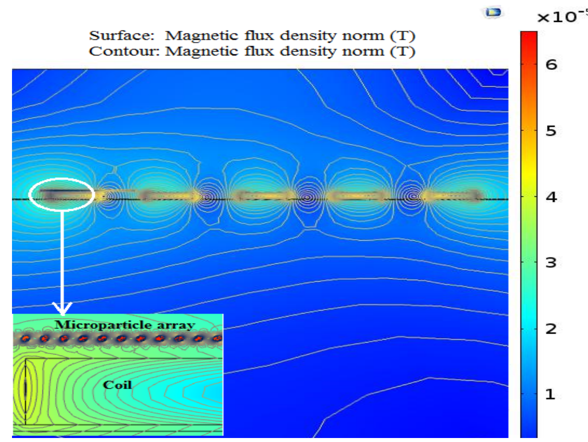

Figure 9. Magnetic flux density distribution along with the microbead-coil interface

The current in the RX coil is simulated by applying a microparticle solution over the coil surface. The applied microparticle solution approximately contains ten iron oxide microparticles. Input currents are varied from 10 μA to 500 μA, and current in the RX coil is simulated for each case, as shown in Fig. 10. The presence of microparticles is found to cause an induced current at the RX coil. The magnetic microparticles modulated the induced current by more than two orders of magnitude.

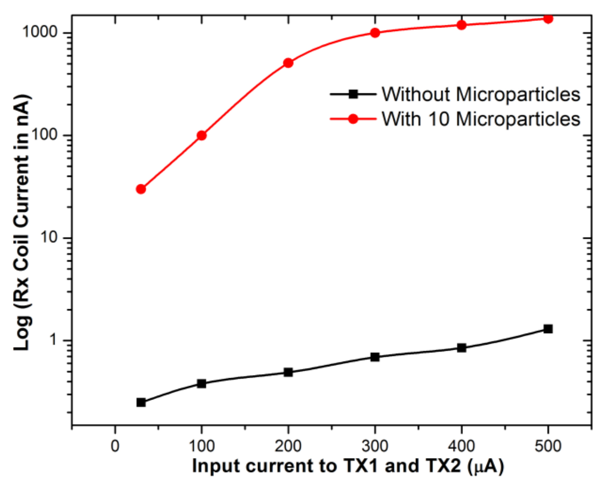

Figure 10. Induced current at the RX coil as a function of the input currents

The performance comparison of various planar coil sensors shown in Table 2 indicates that the proposed induction balance sensor showcases a good detection sensitivity with a better limit of detection and fabrication easiness. The fabrication of the induction-balance sensor requires a single metal level lithography, which is a significant highlight of this design.

The primary performance parameters of a magnetic sensor are its sensitivity and limit of detection [9]. The limit of detection (L_D) of a magnetic sensor is the minimum number of microbeads that can be detected using the sensor. Iron oxide microbeads of 1 µm diameter are taken as the label particles for the induction-balance sensor. Table 2 shows that the induction-balance sensor provides a better limit of detection compared to other planar microcoil based sensors under consideration. The receiving coil current obtained with this limit of detection is 0.1 µA, shown as the sensitivity (*S*) in Table 2. The sensitivity is comparable with the other considered sensors based on planar microcoil. In Table 2, r_p denotes the particle radius in µm. N_M represents the number of metal layers required to fabricate the sensor.

Table 2: Comparison of the induction-balance sensor with some of the existing magnetic biosensors based on planar microcoils

Type of sensor	N_M	Magnetic Particle used	r_p	S	L_D
Spiral coil-based LC coupled oscillator [3]	3	IgG-coated microbead	0.75	0.1 µA	20-30
Resonant spiral coil [10]	3	Dynal M-280	1.4	0.4 µA	10^5
Spiral coils in Bridge configuration [11]	4	Estapor®	0.15 - 0.25	100 pg/mL of the antibody	10^3
This work	1	Fe_2O_3	0.5	0.1 µA	10

Conclusions

A magnetic sensor based on non-spiral planar microcoils using the induction balance principle is studied. The resulting magnetic field distribution and output current are analyzed. The induction-balance sensor is found to produce the highest sensing currents of the order of micro Amperes with a better limit of detection of 10 particles. Fabrication easiness is another advantage of the induction-balance sensor. It requires only a single metal level for microfabrication. In contrast, a conventional planar microcoil based sensor requires a minimum of two metal levels. An improved sensing current can be obtained with amplifier circuits, which is the future scope of this work.

References

1. J. Geng, L. Zhang, C. Zhu, L. Dai, X. Shi and H. Qian, "An Oscillator-Based CMOS Magnetosensitive Microarray Biochip with On-Chip Inductor Optimization Methodology," *IEEE Transactions on Microwave Theory and Techniques*, no. **66(5)**, pp.2556-2569 (2018)
2. J. Llandro, J. Palfreyman, A. Ionescu and C. Barnes, "Magnetic biosensor technologies for medical applications: A review," *Medical & biological engineering & computing*, no. **48(10)**, pp. 977-998, (2010)
3. Y. Zheng, N. Shang, P. Haddad and M. Sawan, "A microsystem for magnetic immunoassay based on planar microcoil array," *IEEE transactions on biomedical circuits and systems*, no. **10(2)**, pp. 477-486 (2016)
4. Makiranta, J. Jarkko and J. O. Lekkala, "Modeling and simulation of magnetic nanoparticle sensor," in IEEE Engineering in Medicine and Biology 27th Annual Conference, 2006.
5. J. Geng, L. Zhang, C. Zhu, L. Dai, X. Shi and H. Qian, "An Oscillator-Based CMOS Magnetosensitive Microarray Biochip with On-Chip Inductor Optimization Methodology," IEEE Transactions on Microwave Theory and Techniques, no. **66(5)**, pp. 2556-2569, 2018.
6. Krishnapriya S, Rama S Komaragiri, Suja K.J, "Detection of Magnetic Particles Using Induction-Balance Microsensor Based on Non-Spiral Planar Microcoils," *Proceedings of IEEE SENSORS 2018*, 28th -31st October 2018, Pullman Aero City, New Delhi, India, pp. 1-4.
7. D. Ambruš, D. Vasic and V. Bilas, "Automatic compensation of primary field coupling for a frequency-domain electromagnetic induction sensor. Instrumentation and Measurement Technology Conference," in *IEEE International Instrumentation and Measurement Technology Conference* (2017).
8. Krishnapriya S, Rama S Komaragiri, Suja K J, "Fabrication, Characterisation, and Modelling of a Novel via-less Single Metal Level Magnetic Microcoil Sensor for Biosensing Applications", *Sensors and Actuators A: Physical*, **290**, pp.190-197 (2019)
9. Lacharme, F, C. Vandevyver, M. A. M. Gijs. "Magnetic beads retention device for sandwich immunoassay: comparison of off-chip and on-chip antibody incubation." *Microfluidics and nanofluidics* **7.4**, p.479 (2009)
10. Richardson J, Hill A, Luxton R, Hawkins P. "A novel measuring system for the determination of paramagnetic particle labels for use in magneto-immunoassays". *Biosensors and Bioelectronics*, **16(9-12)**:1127-32 (2001)
11.Tamanaha CR, Mulvaney SP, Rife JC, Whitman LJ. "Magnetic labeling, detection, and system integration," *Biosensors and Bioelectronics*, **24(1)**:1-3 (2008)

Acknowledgments

The authors would like to acknowledge the National Program on Micro and Smart Systems (NPMaSS) for providing licenses of COMSOL Multiphysics 5.3.